Scanning tunnelling microscopy and spectroscopy on organic PTCDA films deposited on

sulfur passivated GaAs(001)

Scanning tunnelling microscopy and spectroscopy on organic PTCDA films deposited on sulfur passivated GaAs(001)

N Nicoara[1], O Custance[1], D Granados[2], J M García[2], J M Gómez-Rodríguez[1], A M Baró[1] and J Méndez[3,4]

[1] Laboratorio de Nuevas Microscopías, Departamento de Física Materia Condensada C-III, Universidad Autónoma de Madrid, E-28049 Madrid, Spain
[2] Instituto de Microelectrónica de Madrid—CSIC, E-28760 Madrid, Spain
[3] Instituto de Ciencia de Materiales de Madrid—CSIC, E-28049 Madrid, Spain

E-mail: javier.mendez@icmm.csic.es

Abstract
Deposition of 3,4,9,10-perylene-tetracarboxylic-dianhydride (PTCDA) on sulfur passivated gallium arsenide S-GaAs(001) surfaces is investigated by scanning tunnelling microscopy and scanning tunnelling spectroscopy. The surface morphology and the film structure are studied for the multilayer growth of the organic molecules. Spectroscopic results for both clean substrate and ordered areas of PTCDA are shown in this work. We have measured I–V plots at different tip–sample distances, avoiding deformation of the organic layer. Under proper experimental conditions, a gap value of 2.2 eV has been measured on PTCDA crystals, in good agreement with the expected value for PTCDA (2.2–2.55 eV).

(Some figures in this article are in colour only in the electronic version)

1. Introduction

Organic/inorganic interfaces are suitable for building and testing new electronic devices that could be used in nanotechnology [1–5]. Organic molecules modify semiconductor density of states, introducing new states in the gap, or inducing other changes in the electronic behaviour. Particularly, this is the case for PTCDA (3,4,9,10-perylene-tetracarboxylic-dianhydride) molecules absorbed on semiconductor surfaces. This system shows a diode-like electronic characteristic and has been extensively studied due to its application in new organic/inorganic devices.

[4] Author to whom any correspondence should be addressed.

Among organic materials, PTCDA presents remarkable properties for use as an organic semiconductor: optoelectronic properties, relative small gap (optical gap: 2.2 eV, transport gap: 2.55 eV) and quasiepitaxial growth on many substrates [5]. Several studies have been made, investigating the formation of thin PTCDA films on metallic substrates: gold [6–9], silver [10–14], nickel [12], copper [15] and graphite [16], and on passivated semiconductor substrates: silicon [17, 18] and gallium arsenide [18–21]. On these surfaces, PTCDA forms ordered layers due to the stronger molecule–molecule interaction with respect to the molecule–substrate interaction. For the PTCDA bulk, two monoclinic polymorphs have been observed, named as the α phase ($a = 3.74$ Å, $b = 11.96$ Å, $c = 17.34$ Å, $\beta = 98.8°$) and the β phase ($a = 3.87$ Å, $b = 19.30$ Å, $c = 10.77$ Å, $\beta = 83.6°$). PTCDA thin films grow preferentially in the (102) plane, with two quasi-coplanar molecules per cell [5].

Using scanning tunnelling spectroscopy (STS) the electronic properties of molecular films have been investigated over the last few years for a variety of organic materials [9, 22, 23]; valuable information on these electronic properties can be obtained from current–voltage characteristics. Moreover, models for the interpretation of the spectroscopic results have been proposed in terms of the voltage distribution through the organic material [24] or by polarization effects [22].

In this work we study the substrate morphology of PTCDA films by scanning tunnelling microscopy (STM). We compare the results obtained by means of STS [25, 26] on clean gallium arsenide substrate and on organic PTCDA films grown on sulfur passivated GaAs(001). These spectroscopic results, in the absence of a complete theory of electronic transport through organic/inorganic interfaces, bring a new contribution to the understanding of organic/inorganic semiconductors.

2. Experimental details

Experiments were performed in an ultra-high vacuum (UHV) system equipped with surface analysis techniques such as low energy electron diffraction (LEED), Auger electron spectroscopy, sample and tip preparation facilities and evaporators for organic molecular beam epitaxy (OMBE). The system consists of two chambers, one for sample preparation and another for STM analysis [27], connected via a magnetic transfer rod. The base pressure in both chambers is below 1×10^{-10} Torr during STM experiments. A quadrupolar mass spectrometer (QMS) is used for controlling the residual gas and the purity of the evaporating materials. Samples are n-type GaAs(001) provided by Freiberger compounds (Si doped $1–4 \times 10^{18}$ cm^{-3}).

The initial preparation of the substrate [28, 29] was performed in a different chamber with MBE facilities. In this system, after desorption of the native oxide, regrowth of 0.5 μm GaAs (Si doped 2×10^{18} cm^{-3}) with controlled gallium and arsenic fluxes was performed. MBE grown GaAs(001) samples capped with a thick As layer were then transferred to the STM system. After thermal desorption of the As cap at about 300 °C and annealing to 450 °C, for 10 min, an As-terminated (2 × 4) surface was observed by LEED. To obtain sulfur passivated surfaces, the samples were exposed to sulfur flux from a SnS$_2$ evaporator. Final annealing at 500 °C removed sulfur excess from the sample, achieving sulfur terminated GaAs [30]. On to these surfaces PTCDA films were grown by thermal evaporation (OMBE) from purified organic material. The molecules were deposited at various substrate temperatures at a rate of approximately 0.04 ML s^{-1} as determined with a quartz crystal microbalance.

Before the STM/STS experiments were performed, tips were prepared by thermal annealing, field emission and self-sputtering, until stable field emission currents were obtained.

Reproducible results were obtained after *in situ* tip treatment [31] and using tips that provide low-resolution images.

Spectroscopic results were obtained by measuring and averaging $I-V$ plots at selected points. Two types of measurements were performed: the first, by increasing the set-point current to reduce the tip–sample distance and the second one, by direct distance variation. This second type was performed starting with fixed feedback settings (I, V). Then, with opened feedback, the tip was moved towards the sample a certain distance Z (between 0 and 7 Å) while acquiring the $I-Z$ curve. At the end of the approach an $I-V$ curve was recorded. Then the tip was withdrawn to recover the initial parameters.

In order to extract the information from the data, $I-V$ characteristics are presented in three different ways: (a) the $I-V$ characteristic (b) the logarithmic representation and (c) the normalized derivative [32], which is approximately proportional to the local density of states (LDOS). From the comparison between $I-V$ curves obtained over the same points, a maximum limit for the gap is obtained from the logarithmic representation of the $I-V$ characteristics. Similar values for the gap can be obtained in the normalized derivative from the FWHH (full width at half-height) between maxima of the edge peaks.

3. STM results

MBE growth of GaAs(001) performed under the conditions described above leads to an As-terminated surface exhibiting a (2×4) reconstruction. STM images of this surface are obtained using negative sample bias with respect to the tip. We have observed that tunnelling in the sample empty states (at positive bias) is unstable, and no resolution for the As-rich surface (2×4) reconstruction was obtained. Figure 1(a) shows a typical STM image of the (2×4) reconstruction, where rows along the [$\bar{1}$10] direction are observed at two different atomic layers. Models for this reconstruction have been previously reported by other authors [33]. The brighter features observed in the image possibly correspond to an excess of As. Higher resolution images, such as that presented in figure 1(b), show the dimer rows with periodicity 16.9 Å along [110] and periodicity 8.4 Å along [$\bar{1}$10] in good agreement with the expected values of 16 and 8 Å [33]. A profile along the [110] direction is also presented in figure 1(c).

Deposition of 7 ML of PTCDA molecules at RT on sulfur passivated GaAs(001) leads to the formation of small crystals which partially cover the surface. Figure 2 shows the sample with several PTCDA ordered structures. On the left side of the image a hexagonal shape crystal is observed. For the rest of the surface surrounding the crystals we cannot conclude whether it is ordered or not, but we observe distinctive features of PTCDA, such as stripes (similar to those observed at the edges of the hexagonal crystal) or fuzzy areas with spikes. Considering these areas between the crystals as covered with PTCDA, we presume that the overall growth mode of PTCDA films can be assigned to the Stranski–Krastanov mode.

Further deposition of 7 ML more of PTCDA with the sample temperature hold at 180 °C increases the size of the crystals. On the crystals terraces we observe ordered PTCDA molecules corresponding to the herring-bone structure reported for this material. Measuring the distances of the unit-cell, we obtain 18.0 and 12.6 Å, close to the values of the (101) plane of the α-PTCDA phase (18.28 and 11.96 Å) or the β-PTCDA in the (102) plane (19.30 and 12.45 Å) [5]. In figure 3 we present STM images obtained on ordered PTCDA areas. Figure 3(a) shows PTCDA terraces with different orientations. Figure 3(b) corresponds to a higher resolution image where the unit-cell of the herring-bone structure is marked. One of the molecules of the unit-cell appears slightly deeper, producing the stripe-like aspect of the PTCDA terraces in the images.
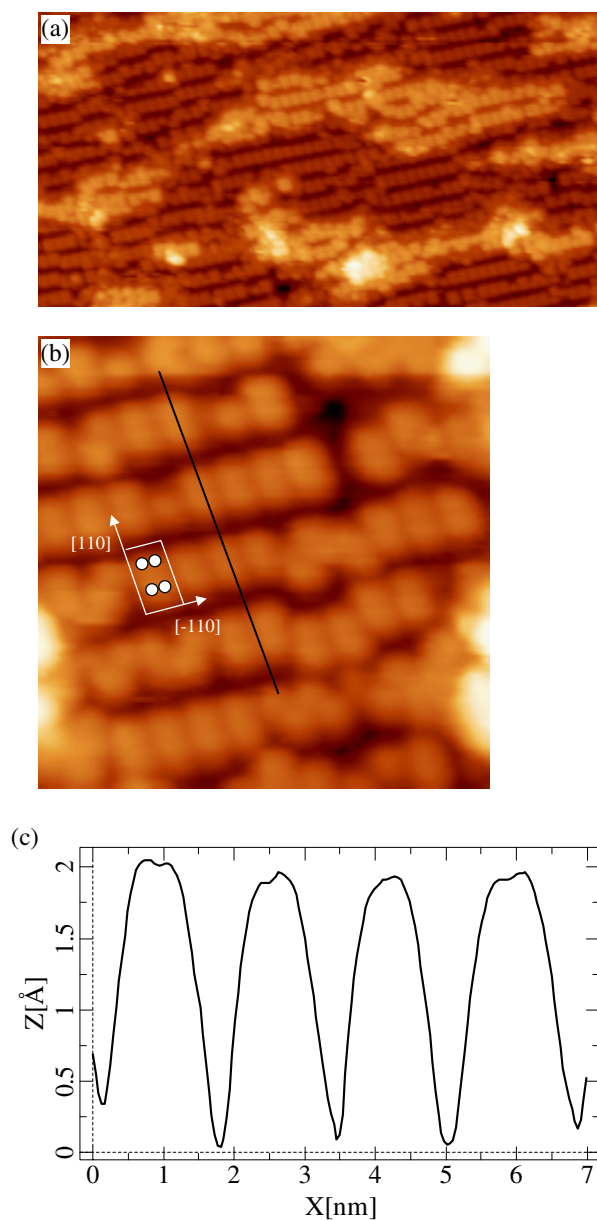
Figure 1. STM images on GaAs(001) prepared by *ex situ* MBE. (a) Terraces showing As rows along the [$\bar{1}$10] direction corresponding to the (2×4) substrate reconstruction (45 nm × 24 nm, $I =$ 2.0 nA, $V = -3.0$ V); (b) higher resolution image (10 nm × 10 nm, $I = 1.0$ nA, $V = -3.0$ V) where the unit-cell and dimers have been marked; (c) profile along [110] direction.

4. STS results

4.1. Comparison between substrate and organic layer

Spectroscopy on the GaAs(001) has been performed previous to sulfur passivation and PTCDA deposition. Figure 4(a) shows I–V plots for three different set-point currents obtained on the
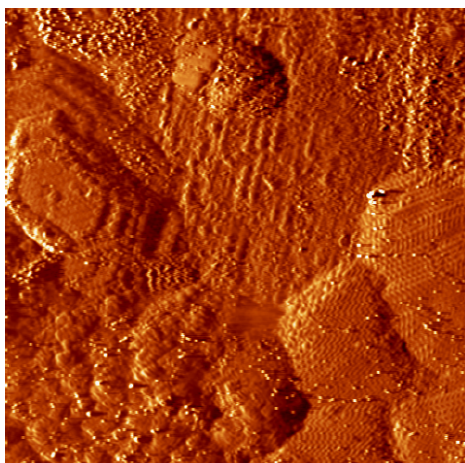
Figure 2. STM image (100 nm × 100 nm, $I = 0.07$ nA, $V = -3.0$ V) in derivative mode obtained after deposition of 7 ML PTCDA. Ordered areas forming PTCDA crystals appear at the right and left sides of the image. At the centre-top, lines of molecules can be observed, denoting that PTCDA covers most of the surface between the crystals.
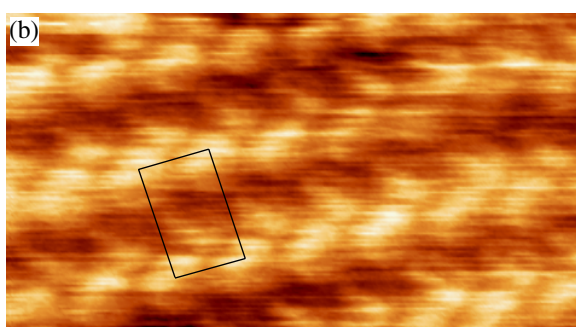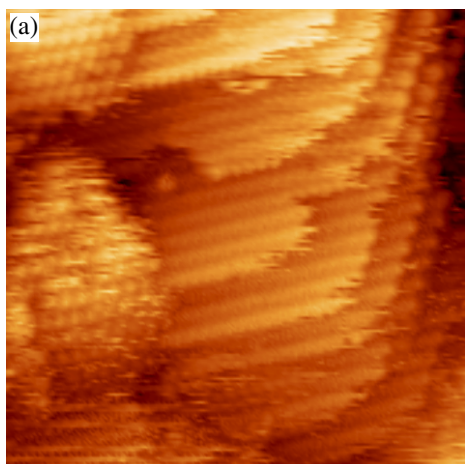

Figure 3. STM images ($I = 0.08$ nA, $V = -3.3$ V) after deposition of 14 ML PTCDA at 180 °C. (a) PTCDA crystal with molecules at the terraces in the herring-bone arrangement (44 nm × 44 nm); (b) Detail (10 nm × 5.8 nm) showing the disposition of the organic molecules.
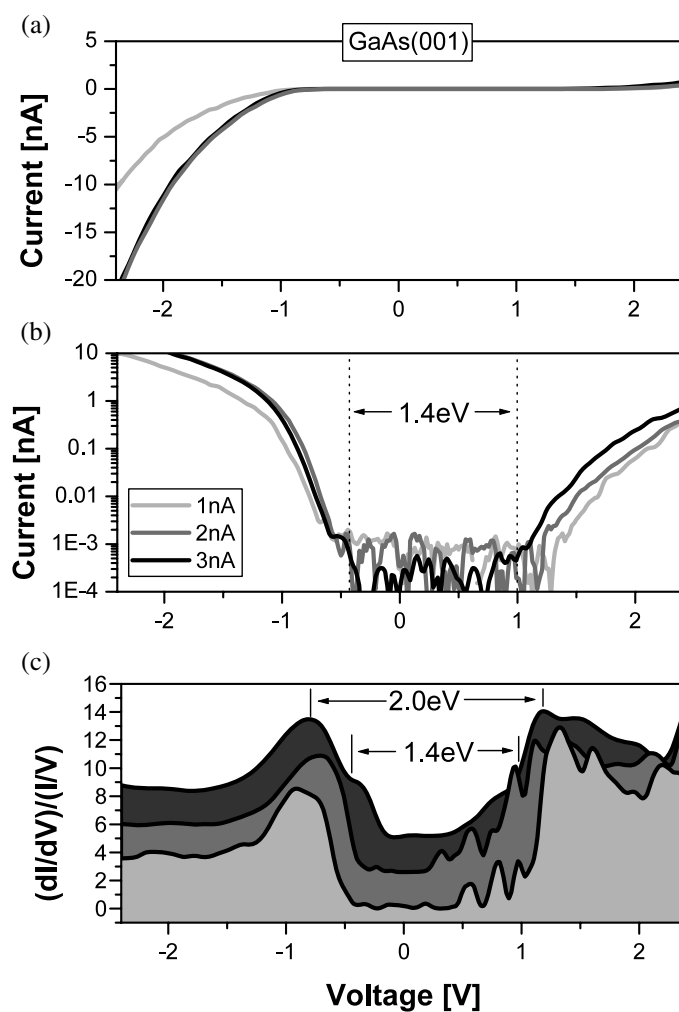
Figure 4. Spectroscopic data obtained for three different set-point currents (1–3 nA, $V = 3.0$ V) on clean GaAs(001) substrate. (a) I–V characteristic; (b) logarithmic representation, where a limit value for the gap of 1.4 V can be measured; (c) normalized derivative, showing peaks at the band edges. The plots are vertically displaced.

clean GaAs substrate. The plots show the typical semiconductor behaviour, but with a deviation towards positive values (although the shift is expected to negative values for an n-type sample). A value for the GaAs gap is obtained from the logarithmic representation (figure 4(b)). Close to zero voltage, the noise level of our experimental setup (of the order of 1 pA) can be observed. A limit value for the gap can be taken from the 1 pA interval (marked in figure 4(b)). The expected value of 1.4 eV [34] is reached for the smallest tip–sample distance (at a set-point current of 3 nA). In figure 4(c) we represent the normalized derivative where similar values for the gap are obtained from the FWHH between maxima of the peaks.

We have recorded spectroscopic curves for the PTCDA/S-GaAs(001) system on top of the PTCDA crystals. Following a similar procedure as for the clean gallium arsenide, the I–V plots over PTCDA ordered areas show semiconducting behaviour. These spectroscopic results
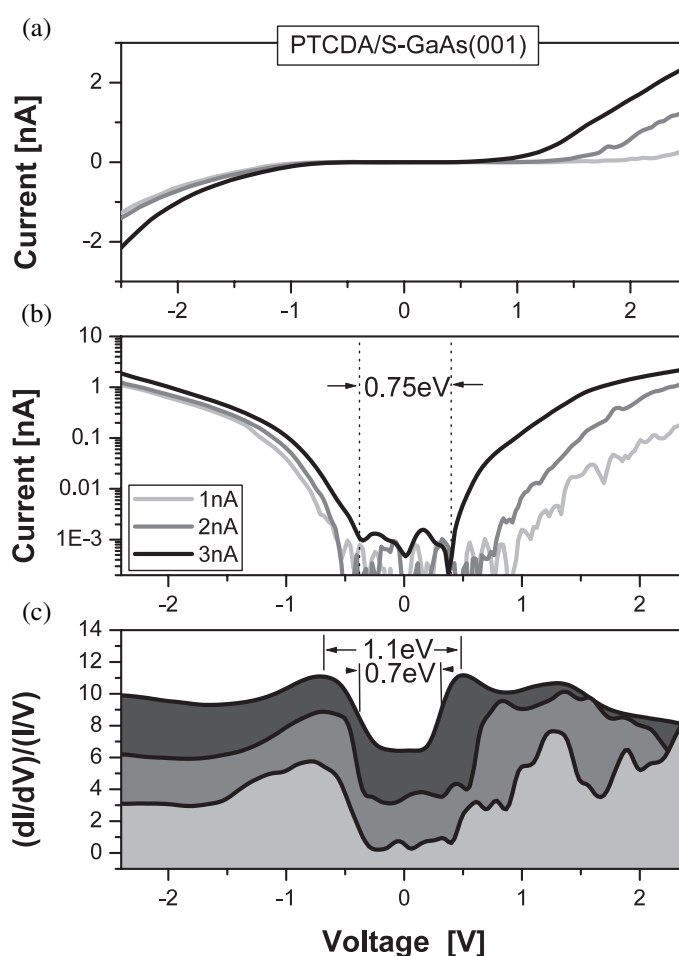
Figure 5. Spectroscopy measured on PTCDA deposited on sulfur passivated GaAs(001). (a) I–V plots measured at different set-point currents (1–3 nA, $V = 3.0$ V); (b) the measured gap value is 0.75 eV; (c) normalized derivative where a peak at positive voltages shifts towards the Fermi level when the current is increased. The plots are vertically displaced.

show more symmetrical curves for the PTCDA in comparison with the substrate. This has been previously observed for other organics systems [35]. The gap value of 0.75 eV obtained in the logarithmic representation at 3 nA (figure 5(b)), is far from the gap values corresponding to the GaAs (1.4 eV) and PTCDA (2.2–2.55 eV). In the normalized derivative plot (figure 5(c)), a peak at positive voltages appears to shift towards the Fermi level as the set-point current increases (the tip–sample distance decreases).

The small value of the gap is quite unexpected. In order to ensure that this corresponds to a real reduction of the gap when the PTCDA forms ordered crystals on the S-GaAs(001) surface, we performed direct measurements of the dependence of the tunnel current on tip–sample distance at fixed tunnel voltage (I–Z plots). These measurements showed a non-exponential behaviour and/or too low values of the apparent tunnel barrier height. Such effects can occur in STM when very strong interactions (or even contact) between tip and sample exist. This leads us to reconsider the way to acquire the I–V plots.
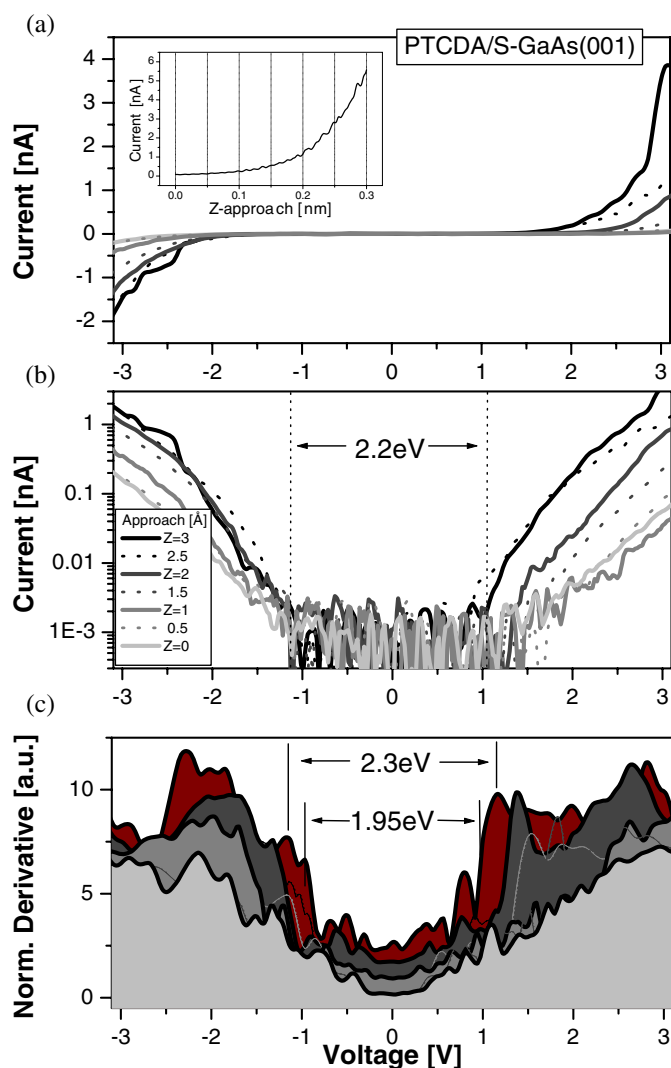
(a)

(b)

(c)

Figure 6. Spectroscopic data measured on PTCDA as in figure 5, but ensuring that the *I*–*Z* variation is exponential. Initial feedback parameters are *I* = 0.08 nA, *V* = −3.2 V. (a) *I*–*V* plots were measured at different approaching *Z* distances. Inset: *I*–*Z* variation showing the exponential behaviour; (b) logarithmic representation where a limit value for the PTCDA gap of 2.2 eV is measured; (c) normalized derivative. The plots are vertically displaced.

Therefore, first we stabilize the feedback at lower tunnel current set-points in order to increase the starting tip–sample distance. Second, we record the *I*–*Z* plot when reducing the tip–sample distance After checking that the current increases exponentially with the distance (see inset in figure 6(a)), we measure *I*–*V* curves at different distances in a range 0–7 Å. When the current–distance plot becomes non-exponential, we consider that there is an interaction with the organic layer and we stop the procedure. In figure 6 we present a set of results for different distances (0–3 Å), where the limit value of the PTCDA gap of 2.2 eV is obtained for the smallest tip–sample distance (before leaving the exponential variation). As in the other case, the curves present a more symmetrical behaviour in comparison with the substrate.

5. Discussion

From the STM results, we conclude that the PTCDA grows on the sulfur passivated gallium arsenide forming ordered crystals with similar structure as the PTCDA bulk. The PTCDA crystals present flat terraces with a herring-bone arrangement.

Spectroscopy on clean GaAs(001) shows a displacement of the $I-V$ plot towards positive values. This aspect has already been observed for n-type (001) semiconductor surfaces [36, 37], and can be correlated to the pinning induced by defects. The gap value measured on the logarithmic representation approaches the expected value 1.4 eV for the closest tip–sample distance. The slight variation of the measured gap value with the distance can be interpreted as an effect of the STS acquisition [38].

On PTCDA covered substrate, spectroscopic measurements exhibit diverse results. For the first acquisition procedure of the current–voltage curves (successive $I-V$ plots as the current is increased) we observe a reduction of the band-gap with the distance. At the highest set-point current (the smallest tip–sample distance) the gap is 0.75 eV. In the normalized derivative a peak localized at positive values (empty states) displaces towards the Fermi level producing more symmetrical $I-V$ curves. As the current–distance dependence showed a non-exponential behaviour, we deduce that the tip is contaminated or that the tip–sample system is not in the tunnel regime. Since we have observed these results for all tip conditions and special care was taken for the tip preparation before and during the experiments, we conclude that there is a strong interaction between the tip and the organic layer.

The second acquisition procedure ($I-V$ plots as the tip approaches the sample), allows us direct identification of the tunnel conditions state from the $I-Z$ variation. From the $I-Z$ curve is possible to see whether the tip is in contact with the organic layer, or contaminated. For normal tunnel conditions, with a clean tip and without touching the organic layer, the current–distance variation exhibits exponential behaviour. For these situations we obtain gap values ($\sim$2.2 eV) in good agreement with the expected value for PTCDA (2.2–2.55 eV). The variation of the gap values with the distance (observed in figure 6) can be explained as an STS-measurement effect, similar to the one observed for the GaAs substrate.

Observing the current behaviour, we ensure that there is no contact between the tip and the organic layer and that we keep in the tunnel regime. Furthermore, when we move the tip towards the sample so much that the current–distance variation ($I-Z$) departs from exponential behaviour, the measured gaps are small, similar to the ones obtained with the first procedure. In figure 7 we present the current variation when the tip is moved 7 Å towards the sample. The plot deviates from exponential behaviour at around 4 Å. Two $I-V$ plots acquired at 3 and 7 Å approach distances are shown in the logarithmic representation. The measured gap values are 2.35 and 0.7 eV respectively. The first one corresponds to the expected value of the PTCDA gap, while the second one is indicative of a strong interaction between the tip and the organic layer, or a possible contact between them. The distance where the I/Z plot deviates from the exponential can be taken as a value for the distance between tip and the organic layer at the initial tunnel conditions. Over this value, the deformation of the organic material has to be taken into account for the interpretation of small values of the gap.

6. Conclusions

The organic/inorganic semiconductor system consisting of PTCDA deposited on sulfur passivated S-GaAs(001), has been studied by scanning tunnelling microscopy and spectroscopy (STM/STS). PTCDA deposition on S-passivated GaAs(001) samples shows crystalline growth with bulk-like structure. In order to obtain the information on the organic/inorganic system,
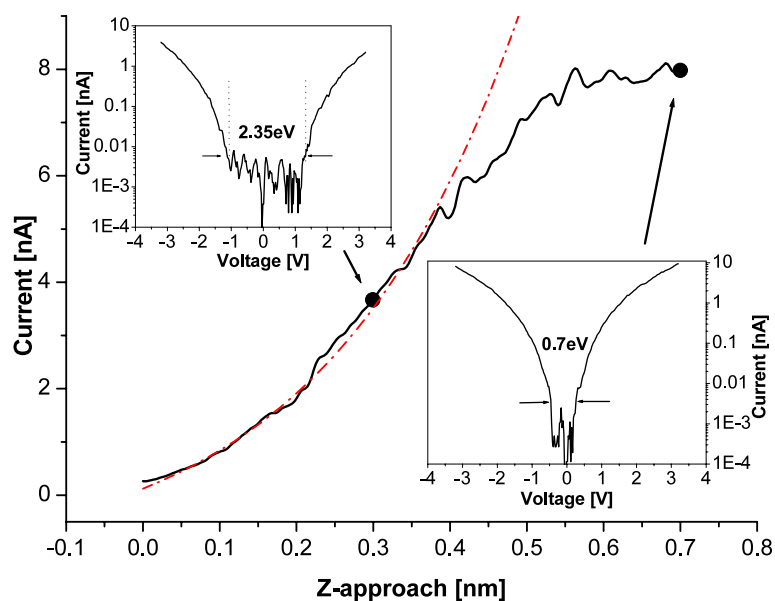
Figure 7. Current versus tip–sample distance curve (I–Z) showing the deviation from the exponential behaviour at an approach distance of 4 Å. Initial feedback parameters $I = 0.26$ nA, $V = -3.2$ V. Insets: two I–V plots in logarithmic representation acquired at 3 and 7 Å, corresponding to exponential and non-exponential behaviour respectively. The measured gap values are 2.35 and 0.7 eV respectively. The tip–sample distance at the initial tunnel conditions deduced from this experiment is 4 Å.

we propose measuring I–V plots at different distances, while observing that the current increases exponentially when moving the tip towards the sample. With this method, avoiding a strong interaction between the tip and the organic layer, we have obtained a value of 2.2 eV from spectroscopic results for the PTCDA gap. We suggest that such strong interactions (or even deformations of the organic layer) could lead to the measurement of anomalously low apparent gap values.

Acknowledgments

References

[1] Torsi L, Dodabalapur A, Rothberg L, Fung A and Katz H 1996 *Science* **272** 1462
[2] Garnier F, Hajlaoui R, Yassar A and Srivastava P 1994 *Science* **265** 1684
[3] Burroughes J H, Bradley D, Brown A, Marks R, Mackay K, Friend R, Burns P and Holmes A 1990 *Nature* **347** 539
[4] Sheats J R, Antoniadis H, Hueschen M, Leonard W, Miller J, Moon R, Roitman D and Stocking A 1996 *Science* **273** 884
[5] Forrest S R 1997 *Chem. Rev.* **97** 1793

[6]   Schmitz-Hübsch T, Fritz T, Sellam F, Staub R and Leo K 1997 *Phys. Rev.* B **55** 7972
[7]   Staub R, Toerker M, Fritz T, Schmitz-Hübsch T, Sellam F and Leo K 2000 *Surf. Sci.* **445** 368
[8]   Gerstenberg M C, Schreiber F, Leung T Y B, Bracco G, Forest S R and Scoles G 2000 *Phys. Rev.* B **61** 7678
[9]   Toerker M, Fritz T, Proehl H, Sellam F and Leo K 2001 *Surf. Sci.* **491** 255
[10] Umbach E, Sokolowski M and Fink R 1996 *Appl. Phys.* A **63** 565
[11] Seidel C, Awater C, Liu X D, Ellerbrake R and Fuchs H 1997 *Surf. Sci.* **371** 123
[12] Umbach E, Glöcker K and Sokolowski M 1998 *Surf. Sci.* **402–404** 20
[13] Glöcker K, Seidel C, Soukopp A, Sokolowski M, Umbach E, Böhringer M, Berndt R and Schneider W D 1998
        Surf. Sci. **405** 1
[14] Shklover V, Tautz F S, Scholz R, Sloboshanin S, Sokolowski M, Schaefer J A and Umbach E 2000 *Surf. Sci.*
        454–456 60
[15] Stöhr M, Gabriel M and Möller R 2002 *Surf. Sci.* **507** 330
[16] Kendrick C, Kahn A and Forrest S R 1996 *Appl. Surf. Sci.* **104/105** 586
[17] Scholz R, Kobitski A Yu, Kampen T U, Schreiber M, Zahn D R T, Jungnickel G, Elstner M, Sternberg M and
        Frauenheim Th 2000 *Phys. Rev.* B **61** 13659
[18] Tenne D A, Park S, Kampen T U, Das A, Scholz R and Zahn D R T 2000 *Phys. Rev.* B **61** 14564
[19] Hirose Y, Forest S R and Kahn A 1995 *Appl. Phys. Lett.* **66** 944
[20] Kendrick C and Kahn A 1998 *Surf. Rev. Lett.* **5** 289
        Kendrick C and Kahn A 1998 *Appl. Surf. Sci.* **123** 405
[21] Nicoara N, Cerrillo I, Xueming D, García J M, García B, Gómez C, Méndez J and Baró A M 2002 *Nanotechnology*
        13 352
[22] Tsiper E V, Soos Z G, Gao W and Kahn A 2002 *Chem. Phys. Lett.* **360** 47
[23] Rinaldi R, Cingolani R, Jones K M, Baski A A, Morkoc H, Di Carlo A, Widany J, Della Salla F and Lugli P 2001
        Phys. Rev. B **63** 75311
[24] Datta S, Tian W, Hong S, Reifenberger R, Henderson J I and Kubiak C P 1997 *Phys. Rev. Lett.* **79** 2530
        Tian W, Datta S, Hong S, Reifenberger R, Henderson J I and Kubiak C P 1998 *J. Chem. Phys.* **109** 2874
[25] Wiesendenger R 1994 *Scanning Probe Microscopy and Spectroscopy* (Cambridge: Cambridge University Press)
[26] Feenstra R M 1994 *Surf. Sci.* **299/300** 965
[27] Home-made bettle STM with NanotecElectrónica WSxM software (http://www.nanotec.es/)
[28] Boubeta C M, Menendez J M, Costa-Krämer J L, Garcia J M, Anguita J V, Bescos B, Cebollada A, Briones F,
        Chernych A V, Malikov I V and Mikhailov G M 2001 *Surf. Sci.* **482** 910
[29] Jackson M D, Thorton J M C, Woolf D A and Weightman P 1996 *Surf. Sci.* **352–354** 724
[30] Zahn D R T, Kampen T U, Hohenecker S and Braun W 2000 *Vacuum* **57** 139
[31] Feenstra R M and Mårtensson P 1988 *Phys. Rev. Lett.* **61** 447
[32] Feenstra R M *et al* 1987 *Surf. Sci.* **181** 295
[33] Hashizume T, Xue Q K, Zhou J, Ichimiya A and Sakurai T 1994 *Phys. Rev. Lett.* **73** 2208
        Hashizume T, Xue Q K, Ichimiya A and Sakurai T 1995 *Phys. Rev.* B **51** 4200
[34] Levinshtein M, Rumyantsev S and Shur M (ed) 1999 *Handbook Series on Semiconductors Parameters* vol 2
        (Singapore: World Scientific)
[35] Tian W, Datta S, Hong S, Reifenberger R, Henderson J I and Kubiak C P 1998 *J. Chem. Phys.* **2874** 109
[36] Kasai S, Negoro N and Hasegawa H 2001 *Appl. Surf. Sci.* **175–176** 255
[37] Lin H, Jaccodine R J and Freund M S 1998 *Appl. Phys. Lett.* **73** 2462
[38] Feenstra R M, Stroscio J A and Fein A P 1987 *Surf. Sci.* **181** 295